

SMECTITE QUASICRYSTALS IN AQUEOUS SOLUTIONS AS A FUNCTION OF CATIONIC SURFACTANT CONCENTRATION

SATORU KUWAHARADA^{1,*}, HIROSHI TATEYAMA², SATOSHI NISHIMURA² AND HIDEHARU HIROSUE³

¹Kagoshima Prefecture Institute of Industrial Technology, 1445-1, Oda Hayato-cho, Aira-gun, Kagoshima Prefecture, 899-5105 Japan

²National Institute of Advanced Industrial Science and Technology, Shuku-machi, Tosu city, Saga Prefecture, 841-0052 Japan

³Cooperative Research Center Kumamoto University, 2081-7 Tabaru, Mashiki-machi, Kamimashiki-gun, Kumamoto Prefecture, 861-2202, Japan

Abstract—Quasicrystals of synthetic fluoromagnesian smectite (FMS) in dodecyltrimethylammonium chloride (DTAC) solutions were investigated as a function of the DTAC concentration by wet type X-ray diffraction (XRD) ζ potential measurements, and dispersion and coagulation (DC) tests. The FMS had an electronegative potential and it was dispersed randomly in an aqueous suspension without DTAC. When the DTAC concentration was 0.002 mol/dm³, FMS tactoids started to develop a structure in which the layer thickness was 1.85 nm. At the isoelectric point, the DTAC concentration was 0.012 mol/dm³ and the FMS tactoid formed a regular stacked structure with a 2.25 nm layer thickness. As the ζ potential of FMS changed from negative to positive, the DC test and XRD measurement showed that the FMS association gradually changed from coagulation to dispersion, which indicates that the formation of the bilayer of surfactants on the surface of FMS produces a repulsion between DTA⁺ adsorbed on the silicate layer of the FMS surfaces. When the equilibrium concentration of DTAC in solution exceeded the critical micelle concentration (CMC), the ζ potential of FMS became greater than the previous values. The XRD analysis of this suspension showed that there were two kinds of rational FMS stackings; one has a layer thickness of 3.20 nm, and the other has a layer thickness of 5.45 nm due to an interstratified structure composed of 3.20 and 2.25 nm layers. The interstratified structure was confirmed by the calculated XRD profiles.

Key Words—Calculated XRD Profile, Interstratification, Layer Thickness, Quasicrystal, Stacking Structure, Wet Type XRD, ζ Potential.

INTRODUCTION

Clay minerals, such as montmorillonite and vermiculite, have the ability to form complexes with organic substances. The characterization of these clay-organo complexes was especially difficult in aqueous suspensions. The wet type XRD apparatus to measure the layer stackings of the clay minerals in aqueous solution was developed by Tateyama *et al.* (1997) and the regularly stacked FMS structure in an aqueous suspension was revealed in sodium tripolyphosphate. The FMS has properties similar to montmorillonite which was synthesized by an intercalation process using talc and sodium silicofluoride (Tateyama *et al.*, 1992, 1996). Various analyses with XRD, nuclear magnetic resonance (NMR), magic angle spinning (MAS), and thermogravimetric analysis (TG) were performed in order to establish the formation process of the FMS (Tateyama *et al.*, 1992, 1996; Noma *et al.*, 1997). The quasicrystals of FMS in the suspension were investigated to determine the formation process of the stacked structure of FMS with the increasing cationic surfactant concentrations using wet type XRD apparatus. The electrokinetics, the elution

amount of Na⁺ ions, the amount of adsorbed DTAC and simulations of theoretical XRD line profiles were used to interpret the stacked structure in the suspensions.

EXPERIMENTAL

Sample preparation

Pure FMS was used as the starting material. It has similar physical and swelling properties to a trioctahedral magnesian smectite close to stevensite. The structural formula is Na_{0.66}Mg_{2.68}(Si_{3.98}Al_{0.02})O_{10.02}F_{1.96} and the cation exchange capacity (CEC) is 84.9 meq/100g. The lattice parameters of FMS are $a = 0.524$, $b = 0.908$, $c = 0.970$ nm and $\beta = 100^\circ$. The FMS was obtained from CO-OP Chemicals, Tokyo, Japan. It is commercially available as ME-100F. The DTAC from Katayama Chemicals Industries Ltd, is a reagent-grade chemical. One gram of FMS was added to 100 cm³ of the DTAC solutions as shown in Table 1. Each suspension was stirred for 24 h and then divided into two parts. Firstly, 5 cm³ of the suspension were separated and used for measuring the quasicrystal of FMS using the wet type XRD apparatus. The remaining 95 cm³ of the suspensions were centrifuged twice for 60 min at 10,000 rpm to separate the FMS particles from the suspension. The supernatant was used to analyze the DTAC concentration and the amount of Na⁺ ion elution.

* E-mail address of corresponding author: kharada@kagoshimait.go.jp

Table 1. Experimental conditions.

Sample	Sample symbol	FMS (g)	DTAC (mol/dm ³)	¹ DTAC/ ² FMS
DTAC0	A	1.0	0	0
DTAC002	B	1.0	0.002	0.24
DTAC004	C	1.0	0.004	0.47
DTAC01	D	1.0	0.01	1.18
DTAC02	E	1.0	0.02	2.36
DTAC03	F	1.0	0.03	3.53
DTAC04	G	1.0	0.04	4.71
DTAC1	H	1.0	0.1	11.8

¹ DTAC = concentration of DTAC (mol/100 cm³).

² FMS = CEC of FMS (mol/100 cm³).

(In the case of B, the concentration of DTAC = 0.002 mol/dm³, *i.e.* DTAC = 2.0×10^{-4} mol/100 cm³; the CEC of FMS = 84.9 meq/100 g = 8.49×10^{-4} mol/g, *i.e.* FMS = 8.49×10^{-4} mol/100 cm³. DTAC/FMS = 0.24.)

Wet type XRD measurement

The 5 cm³ sample of the FMS suspension in the presence of DTAC was poured into a sample cell. The bottom of the sample cell was covered with Mylar film 2.5 μm thick (Chemplex X-ray Film Mylar). The sample cell was placed on the sample holder of the XRD instrument. The XRD patterns of the suspensions were measured using Philips X'Pert. The X-ray beam was irradiated from a lower part and the intensity of the diffracted beam was detected from the lower part (Tateyama *et al.*, 1997).

Electrophoretic measurement

The ζ potential of the FMS was measured using a Penkem System 3000. The suspension is too thick to measure the ζ potential, so a small amount of FMS (1 mg) obtained after centrifugation, was mixed with 50 cm³ of supernatant, which had the same DTAC concentration as the suspension. Each sample of the FMS suspensions was dispersed by supersonic waves for 10 min. The ζ potentials of the FMS particles were calculated using the Helmholtz-Smoluchowski equation (Jacob, 1985). The temperature of the sample cell was controlled at $25 \pm 1^\circ\text{C}$.

Test of dispersion and coagulation

A 0.25 g sample of FMS was added to the measuring cylinder and the DTAC solution filled the cylinder up to 25 cm³. The suspensions were dispersed by a supersonic wave for 10 min before starting the experiment, and the coagulation height of the suspension was measured after 24 h.

Quantitative analysis of adsorbed DTAC

The Na⁺ ions, which were replaced by cationic surfactants in the FMS, and the DTAC concentrations, which adsorbed on the silicate surface of the FMS, were analyzed as follows. The amount of Na⁺ was measured

using an HITACHI Z-8000, Polarized Zeeman Atomic Absorption Spectrophotometer. The DTAC concentration in the supernatant was measured using the method described by Takeda and Usui (1987). The DTA⁺ was colored by metanil yellow, and the DTA⁺ that reacted with the metanil yellow was extracted using a chloroform solution. The absorbance spectrum was recorded on a JASCO V-550 UV/VIS Spectrophotometer, and the DTAC concentration was determined using a calibration curve at 407 nm. The concentration of adsorbed DTAC molecules was then estimated by subtraction from the initial DTAC concentration.

RESULTS

XRD measurement

The XRD patterns of the FMS suspensions in different concentrations of DTAC are shown in Figure 1a–h. The XRD pattern in Figure 1a shows no Bragg reflection, which indicates that the FMS was completely delaminated and randomly dispersed in the aqueous solution without DTAC (DTAC0). The 001 reflection at 1.85 nm is recognized in Figure 1b at a DTAC (DTAC002) concentration of 0.002 mol/dm³. This indicates that the face-to-face interaction of FMS occurs with a finite particle distance even in the dilute surfactant solutions. For DTAC004, the 001 reflection at 2.01 nm appears as shown in Figure 1c. Figure 1d shows the XRD pattern for DTAC01. The reflections are sharp giving the series of 001 lines at 2.25 and 1.12 nm and the average basal spacing is 2.25 nm. As the concentration of DTAC increases, the layer thickness of FMS also increases and the intensity of the 001 reflection is strong. Figure 1e shows that the *d*(001) value of the DTAC02 sample is 2.25 nm, which is the same as that of DTAC01, but the intensity of the 001 reflection of DTAC02 becomes weaker than that of DTAC01. The XRD patterns of the samples from DTAC03 to DTAC1 are very similar to those shown in Figure 1f–h.

Electrophoretic properties

The values of the measured ζ potential of the FMS particle are shown in Figure 2. The ζ potential of FMS was −40 mV in the presence of 1×10^{-3} mol/dm³ KCl. In the region from B to C, the ζ potential was almost constant, but in the region C–E, the ζ potential increased rapidly and became an isoelectric point at point D. The DTAC concentration of the isoelectric point was estimated at 1.2×10^{-2} mol/dm³. The DTA⁺ of the cationic surfactants adsorbed on the surface of the FMS until the ζ potential became the isoelectric point. Inasmuch as these organic cations were strongly preferred by the exchange sites over Na⁺, exchange adsorption of the cationic surfactant took place. In the region of E–H, the ζ potential increased from E to G and became constant from G to H.

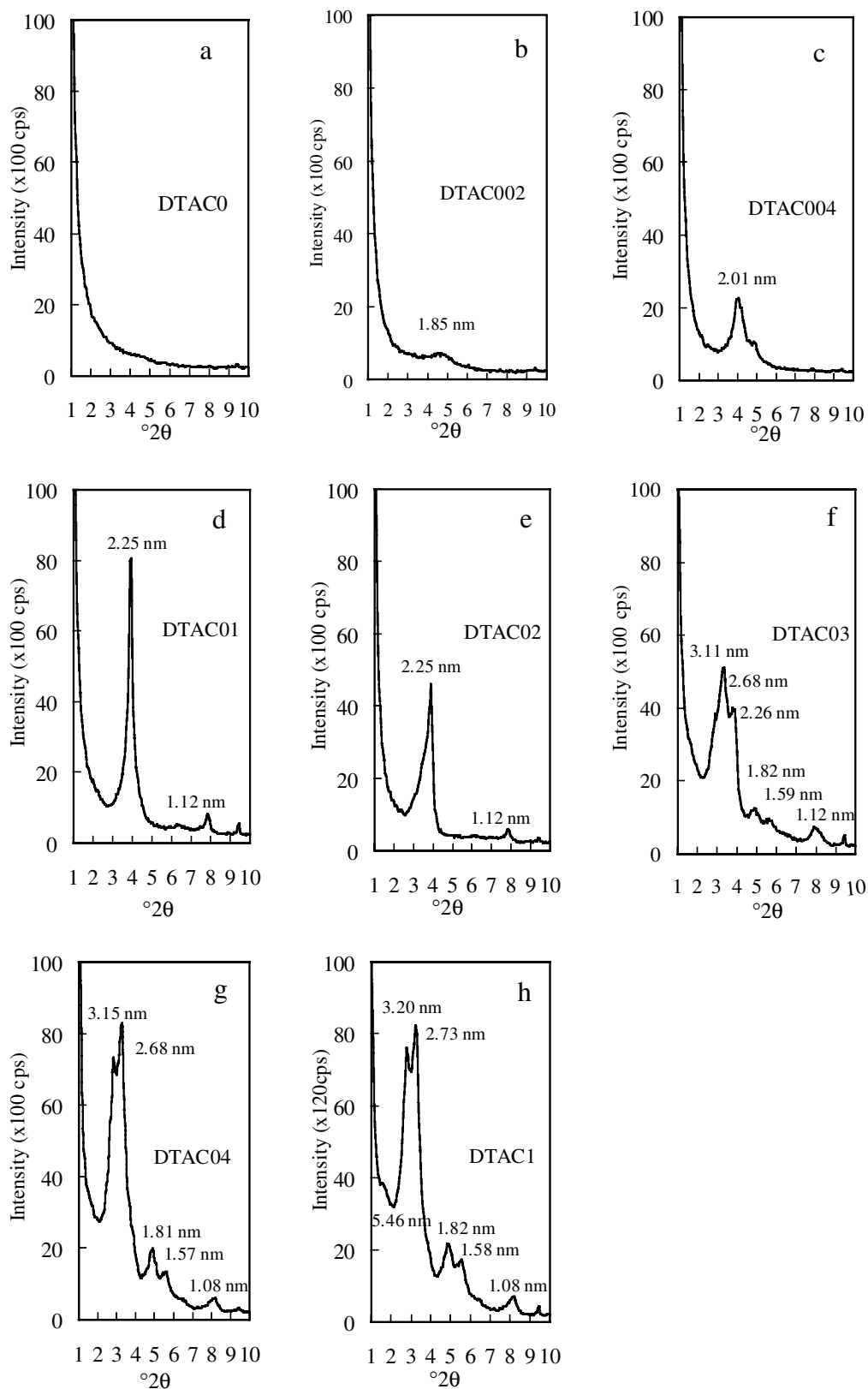


Figure 1. X-ray diffraction patterns of FMS suspensions in different concentrations of DTAC

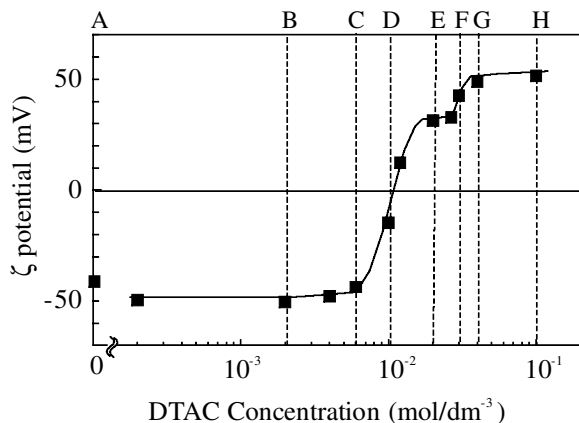


Figure 2. ζ potential of FMS as the function of DTAC concentration.

Test of dispersion and coagulation

The DC test of FMS as a function of the DTAC concentration is shown in Figure 3. The variation phenomenon of the DC test had a similar tendency to the result of the ζ potential measurement. The sedimentation height was at a maximum around D at the isoelectric point. In the region A–C, FMS was dispersed, and FMS was coagulated in the C–D region, but the FMS was slightly redispersed in the D–H region.

Quantitative analysis of adsorbed DTAC

The relationship between the elution amount of Na^+ in the FMS suspension and the DTAC concentration is shown in Figure 4. The concentration of Na^+ is expressed in CEC. The amount of elution (CEC) of Na^+ reached a maximum at point D (isoelectric point). Figure 5 shows the adsorption isotherms of DTAC in the FMS suspension. The DTA^+ adsorption on the FMS surface is also expressed in CEC. The amounts of adsorbed DTA^+ on the FMS surface from B to G were 0.24, 0.47, 1.16, 1.64, 2.23 and 2.49 CEC, respectively.

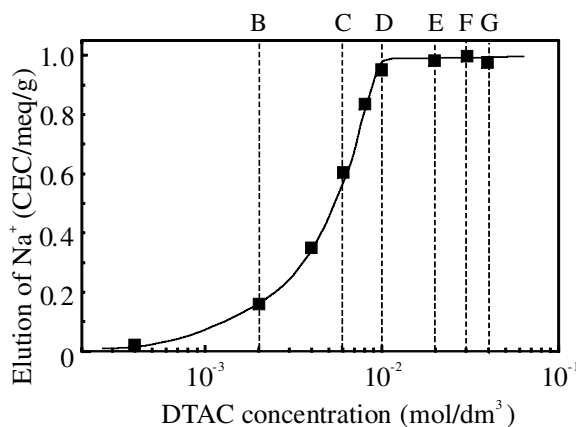


Figure 4. The amount of Na^+ elution in supernatant solutions as a function of the DTAC concentration.

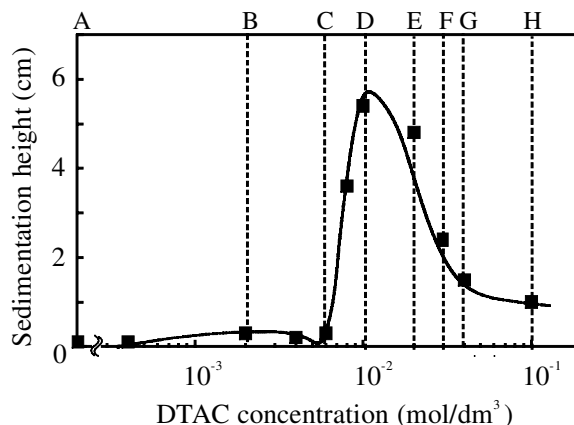


Figure 3. Sedimentation height of FMS suspensions after 24 h in different concentrations of DTAC.

DISCUSSION

Tactoid structures in the A–D region

The FMS particles had a negative ζ potential, -41 mV, and they were completely dispersed in the aqueous suspension at point A. The ζ potential of DTAC002 had a similar negative charge to that of DTAC0, but the XRD pattern indicates that the FMS tactoids started to develop a structure with finite layer spacing. At point D, the tactoid formed a very regular structure with the 2.25 nm layer thickness.

The calculated specific surface area of the FMS is $750 \text{ m}^2/\text{g}$. The ideal number of the adsorption sites, at which DTA^+ can adsorb on the FMS surface, was calculated to be 1.04×10^{18} site/ m^2 from the structural formula, including nearly 28% non-exchangeable Na^+ (Tateyama *et al.*, 1998) and the specific area. Using the DTA^+ concentration ($1.2 \times 10^{-2} \text{ mol}/\text{dm}^3$) at the isoelectric point, the real number of adsorption sites was calculated to be 0.96×10^{18} site, which corresponds roughly to the ideal number of adsorption sites (1.04×10^{18} site).

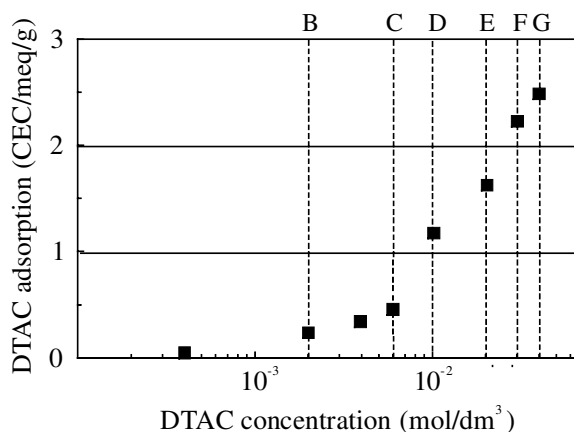


Figure 5. Adsorption isotherm of DTAC in the FMS suspensions.

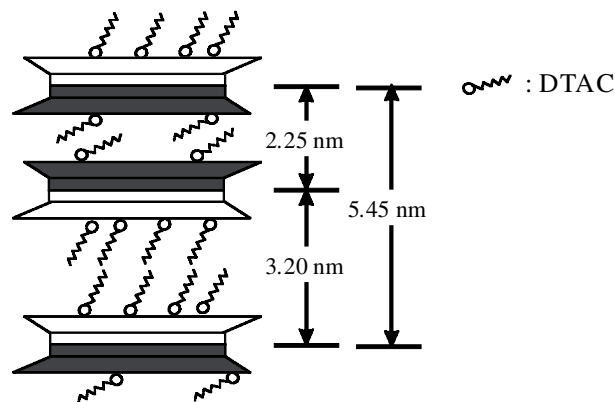


Figure 6. Schematic representation of interstratified structure consists of 3.20 and 2.25 nm layers in the suspension.

Tactoid structure including the interstratified structure in the D–H region

The ζ potential turns positive by forming a bilayer of adsorption of DTAC on the FMS surface from D to E. Part of the tactoid structure may have collapsed, because the intensity of the 001 reflection of DTAC02 became weak compared with that of DTAC01. In the F–H region in which the equilibrium concentration in the solution exceeded the CMC, the cationic surfactant adsorbed in excess because the ζ potential became greater than that of the previous region. The suspensions from DTAC03 to DTAC1 showed very complicated XRD patterns. After consideration of many kinds of stacking modes, we estimated that two kinds of stacking modes existed in these tactoids; one had a layer spacing of 3.20 nm, and the other had a layer spacing of 5.45 nm. The tactoids with 3.20 nm layer thickness were considered to have the structure in which DTA^+ was highly adsorbed in the interlayer site. The other structure of parallel aggregated FMS particles with the 5.45 nm layer thickness may have an interstratified structure of 3.20 and 2.25 nm layers.

Interstratified structure

To confirm the interstratified structure above, the theoretical XRD profile was calculated on the basis of the Hendricks and Teller equation (1942). The calculation procedures followed the method of Sato (1987, 1988) and Watanabe (1988). Figure 6 shows the ideal structural model of the regularly interstratified structure for 2.25 and 3.20 nm layers. The calculated profile of CP54 is shown in Figure 7a, in which the calculated structure is based on Reichweite ($R = 1$) using parameters such as $W_{22.5}$ (existence probability of 22.5 nm layer) = 0.55, $W_{32.0}$ (existence probability of 32.0 nm layer) = 0.45, and $P_{22.5-32.0}$ (continuing probability of these two layers) = 0.90. Figure 7b shows the calculated profile (CP32) of the monolayer structure with a 3.20 nm layer thickness. The sum profile of CP32 and CP54 is shown in Figure 7c. This

result indicates that the calculated XRD profile of CP54+CP32 is very similar to the observed pattern as shown in Figure 7d. Therefore, the reflections of one parallel stack of FMS particles are the series of 00 l lines at 5.46, 2.73, 1.82, 1.08 nm and the average basal value is 5.45 nm, and the series of 00 l lines at 3.20, 1.58, 1.08 nm and the average basal value was 3.20 nm. To determine the reason why the FMS has an interstratified structure, the structural properties of DTAC002 were investigated under dry FMS conditions.

The XRD pattern of the oriented DTAC002 on the glass plate is shown in Figure 8a. This specimen exhibited a weak peak at 2.60 nm and a strong peak at

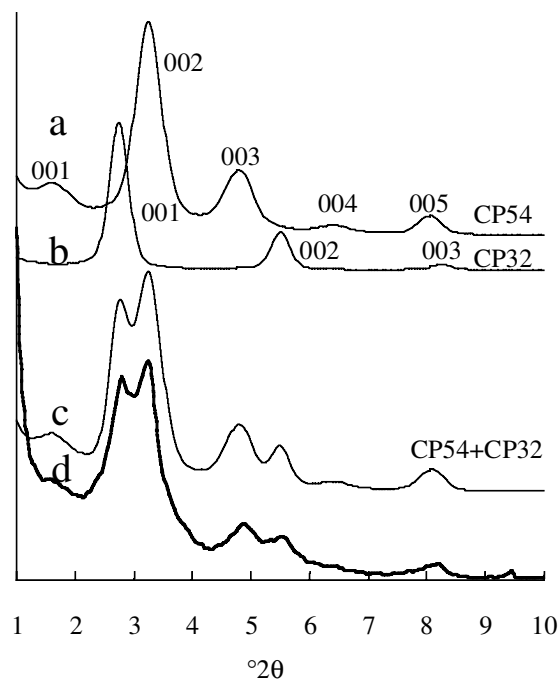


Figure 7. Calculated and observed XRD patterns of DTAC1; (a) CP54: calculated profile on the basis of $R=1$, $W_{22.5} = 0.55$, $W_{32.0} = 0.45$, and $P_{22.5-32.0} = 0.90$; (b) CP32: calculated as monolayer structure with 3.20 nm layers; (c) CP54+CP32: sum profile of CP54 and CP32; (d) observed pattern.

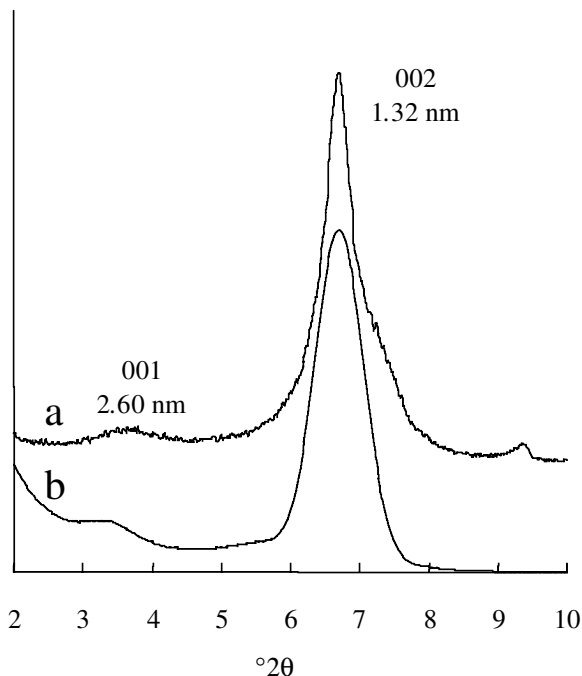


Figure 8. Observed and calculated XRD patterns of oriented DTAC002 measured in dry condition: (a) observed pattern; (b) calculated profile as regularly interstratified structure of 1.40 and 1.25 nm layers.

1.32 nm. Pure FMS under dry conditions usually has a layer thickness of 1.25 nm. The basal spacing of FMS is generally 0.955 nm, measured under a very low humidity, but FMS expands readily by incorporating moisture from the air and then it has a monolayer hydrate with a layer thickness of 1.25 nm. In Figure 8a, the weak peak at 2.60 nm may be ascribed to the regular interstratification of a 1.40 nm layer with a DTA^+ adsorbed silicate layer and the 1.25 nm layer with a monolayer hydrate. Figure 8b shows the theoretical profile of the regularly interstratified structure of 1.40 and 1.25 nm layers based on the ideal structural model as shown in Figure 9. The calculated structure is based on Reichweite ($R = 1$) using parameters such as $W_{1.40}$ (existence probability of 1.40 nm layer) = 0.40, $W_{1.25}$ (existence probability of 1.25 nm layer) = 0.60, and $P_{1.40-1.25}$ (continuing

probability of these two layers) = 0.95. This result indicates that the dried sample of DTAC002 has an interstratified structure of layer thickness 1.40 and 1.25 nm. These facts show that at the low DTA^+ concentrations, DTA^+ starts to be preferentially adsorbed on one side of the tetrahedral sheet of FMS (white part of tetrahedral sheet in Figure 9), but it is not adsorbed on the other (black part). Therefore, DTA^+ can be adsorbed to a high density on one side of silicate layer after CMC. This structural model of FMS agrees well with the previously reported structural model (Tateyama *et al.*, 1998).

CONCLUSIONS

Using DTAC adsorption onto the silicate surface of synthetic fluoromagnesian smectite (FMS) in cationic surfactant (DTAC) solutions, it was found that the FMS formed various tactoid structures, related to the concentration of DTAC. In aqueous suspension without DTAC, the FMS has an electronegative potential and is randomly dispersed. The adsorption of DTA^+ on the FMS surface leads to flocculation and builds a parallel stacked structure, because the DTA^+ adsorbed on the FMS repulse each other in the DTAC solutions. As the amount of adsorbed DTAC increases, the layer thickness increases until the isoelectric point. At the isoelectric point, the FMS tactoid forms a regular stacked structure with 2.25 nm layer thickness. As the ζ potential changes from negative to positive, the FMS redisperses because the FMS surface adsorbs the hydrophobic group of the surfactants having the bilayer form, in which FMS produced a repulsion between the DTA^+ adsorbed on silicate surfaces. When the equilibrium concentration of DTAC in solution exceeds the CMC, there are two kinds of rational stacking. One has 3.20 nm layer thickness and the other has 5.45 nm layer thickness, the latter being the interstratified structure with 3.20 and 2.25 nm layers.

ACKNOWLEDGMENTS

We thank Mr A. Abiko of CO-OP Chemicals, Tokyo, Japan, for treatment of the synthetic fluoromagnesian

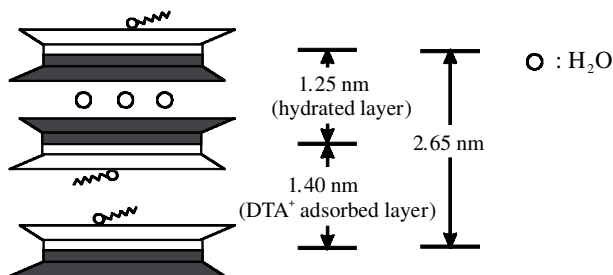


Figure 9. Schematic representation of an interstratified structure of 1.25 and 1.40 nm layers in dry conditions indicating a 2.65 nm superlattice.

smectite (FMS) and Miss T. Chikushi of The National Institute of Advanced Industrial Science and Technology, Tosu, Japan, for measuring the ζ potential.

REFERENCES

- Hendricks, S. and Teller, E. (1942) X-ray interference in partially ordered layer lattices. *Journal of Chemical Physics*, **10**, 147–167.
- Jacob, N.I. (1985) *Intermolecular and Surface Forces*. Academic Press, Tokyo, pp. 111–119.
- Noma, H., Tateyama, H., Nishimura, S. and Inoue, K. (1997) ^{29}Si and ^1H NMR of expandable mica ion-exchanged by NH_4^+ . *Chemistry Letters*, 199–200.
- Sato, M. (1987) Interstratified (mixed layer) structure and their theoretical X-ray powder patterns. I. Theoretical aspects. *Clay Science*, **7**, 1–48.
- Sato, M. (1988) Interstratified (mixed layer) structure and their theoretical X-ray powder patterns. II. In the case of illite/montmorillonite interstratification. *Clay Science*, **7**, 3–88.
- Takeda, S. and Usui, S. (1987) Adsorption of dodecylammonium ion on quartz in relation to its flotation. *Colloids and Surfaces*, **23**, 15–28.
- Tateyama, H., Noma, H., Nishimura, S., Adachi, Y., Ooi, M. and Urabe, K. (1988) Interstratification in expandable mica produced by cation-exchange treatment. *Clays and Clay Minerals*, **46**, 245–255.
- Tateyama, H., Nishimura, S., Tsunematsu, K., Jinnai, K., Adachi, Y. and Kimura, M. (1992) Synthesis of expandable fluorine mica. *Clays and Clay Minerals*, **40**, 180–185.
- Tateyama, H., Tsunematsu, K., Noma, H. and Adachi, Y. (1996) Formation of expandable mica from talc using intercalation procedures. *Journal of the American Ceramic Society*, **179**, 3321–3324.
- Tateyama, H., Scales, P.J., Ooi, M., Johnson, S.B., Rees, K., Boger, D.V. and Healy, T.W. (1997) Effects of particle alignment on the flow properties of an expandable mica in $\text{Na}_5\text{P}_3\text{O}_{10}$ and $\text{K}_4\text{P}_2\text{O}_7$ solutions. *Langmuir*, **13**, 6393–6399.
- Watanabe, T. (1988) The structural model of illite/smectite interstratified mineral and the diagram for its identification. *Clay Science*, **7**, 97–114.

(Received 22 January 2001; revised 23 May 2001; Ms 515)